

Evolution of the Ratio of Strontium-87 to Strontium-86 in Seawater from Cretaceous to Present

JENNIFER HESS, MICHAEL L. BENDER, JEAN-GUY SCHILLING

A detailed record of the strontium-87 to strontium-86 ratio in seawater during the last 100 million years was determined by measuring this ratio in 137 well-preserved and well-dated fossil foraminifera samples. Sample preservation was evaluated from scanning electron microscopy studies, measured strontium-calcium ratios, and pore water strontium isotope ratios. The evolution of the strontium isotopic ratio in seawater offers a means to evaluate long-term changes in the global strontium isotope mass balance. Results show that the marine strontium isotope composition can be used for correlating and dating well-preserved authigenic marine sediments throughout much of the Cenozoic to a precision of ± 1 million years. The strontium-87 to strontium-86 ratio in seawater increased sharply across the Cretaceous/Tertiary boundary, but this feature is not readily explained as strontium input from a bolide impact on land.

AT ANY ONE TIME, THE STRONTIUM isotope composition in seawater is uniform throughout the ocean because the oceanic residence time of strontium (5 million years) (1, 2) is much longer than the mixing time of the oceans (~ 1000 years) (3). During the course of geologic time, the $^{87}\text{Sr}/^{86}\text{Sr}$ in seawater has varied because of changes in the relative fluxes of strontium to the oceans from different sources, each with its own characteristic strontium isotope composition. These include submarine hydrothermal activity (4–7), riverine fluxes (7), and submarine recycling (by limestone recrystallization and erosion of ancient sedimentary carbonate) (7–9). A record of the present and past seawater strontium isotope compositions can be used

to understand the role of the various sources in regulating seawater chemistry. There is increasing recognition that the seawater strontium isotope composition is generally a smoothly varying function of time and can be used for high precision correlations of oceanic sediments for certain time periods (10, 11).

A substantial number of early (12–16) and more recent (7, 10–11) studies have delineated the seawater strontium isotope curve increasingly well. We extend this work by presenting data for the last 100 million years from analysis of strontium isotopes in well-preserved fossil foraminifera from Deep Sea Drilling Project (DSDP) cores. We have improved the resolution of past work by screening to avoid diagenetically altered

samples, by achieving a high analytical precision, and by analysis of a large number of samples at small time intervals.

The cores used (Table 1) were taken from sites with high quality carbonate sequences chosen on the basis of preservation and continuity of the sections, as well as on the availability of ancillary stratigraphic data for age estimates. Generally complete records of foraminiferal $^{87}\text{Sr}/^{86}\text{Sr}$ were obtained from cores with age-overlapping sequences from both the Pacific and Atlantic basins. Cenozoic epochs are represented by at least two overlapping cores; Cretaceous $^{87}\text{Sr}/^{86}\text{Sr}$ records do not overlap.

Fossil foraminifera were separated from sediment samples by standard procedures (17). Mixed planktonic species (whole tests; size fraction, $>150\ \mu\text{m}$) were hand-picked from the samples for isotopic analysis (18). Because the foraminifera contain virtually no ^{87}Rb (the radioactive parent of ^{87}Sr), it is not necessary to age-correct the measured foraminiferal $^{87}\text{Sr}/^{86}\text{Sr}$ ratio for any contribution from the decay of ^{87}Rb since the time of deposition. The accuracy and precision of the analytical method can be evaluated from nine replicate analyses of modern seawater for which we obtained a value of 0.709198 ± 0.000020 (2 standard deviations, Table 2).

Samples were assigned ages on the basis of biostratigraphic zonations in conjunction with the most recent time scale of Berggren *et al.* (19, 20). Within biostratigraphic datum levels, ages were assigned by interpolation. In addition, two sites (502 and 516) were magnetostratigraphically dated (21, 22).

The measured foraminiferal $^{87}\text{Sr}/^{86}\text{Sr}$ ratios reflect the contemporaneous seawater $^{87}\text{Sr}/^{86}\text{Sr}$ only if the foraminifera are pristine or the effects of diagenetic alteration are minimal. Because interstitial waters are open systems that can gain strontium from coexisting aluminosilicates, older and younger sediments, and underlying basalt (23, 24), the pore water strontium isotope composition is generally different from that of the coexisting foraminifera. Diagenesis, therefore, can significantly alter the $^{87}\text{Sr}/^{86}\text{Sr}$ of fossil foraminifera.

We used two criteria to evaluate diagenetic alteration. First, foraminifera were regarded as recrystallized if their Sr/Ca ratios were lower than those of well-preserved contemporaneous samples studied by Graham *et al.* (25) and Delaney (26) (Fig. 1). Diagenesis lowers the Sr/Ca because, at slow precipitation rates associated with recrystallization, the calcite-seawater distribution coefficient

Table 1. Site information for DSDP cores used in this study.

Leg/site	Location	Water depth (m)	Sample age ($\times 10^6$ years)
68/502	Colombia Basin, Western Caribbean 11°29.42'N; 79°22.78'W	3052	0–7
90/593	Lord Howe Rise, Southwest Pacific 40°30.47'S; 167°40.47'E	1068	0.6–40.9
72/516 516F	Rio Grande Rise, South Atlantic 30°16.59'S; 35°17.11'W	1313	5.3–49.0
29/277	Campbell Plateau, Southwest Pacific 52°13.43'S; 166°11.48'E	1214	29.0–33.7
41/366	Sierra Leone Rise, Equatorial Atlantic 3°40.7'N; 9°51.1'W	2853	40.4–59.7
86/577	Shatsky Rise, North Pacific 32°26.51'N; 157°43.40'E	2675	64.0–67.0
32/305	Shatsky Rise, North Pacific 32°00.13'N; 157°51.00'E	2903	39.2–100.9
39/356	Sao Paulo Plateau, South Atlantic 28°17.22'S; 46°05.28'W	3175	66.2–66.5

Graduate School of Oceanography, University of Rhode Island, Narragansett 02882.

of strontium is much less than it is at the rapid precipitation rates associated with formation of biogenic calcite (27). Second, samples were thought to be recrystallized if examination by scanning electron microscopy revealed euhedral calcite crystals, cementation or other overgrowths. As a further check, the isotopic composition of pore water strontium was measured in samples from DSDP sites 516, 593, and 305 (Table 3 and Fig. 2). Where pore water $^{87}\text{Sr}/^{86}\text{Sr}$ ratios are close to those of coexisting foraminifera, minor diagenesis would be inconsequential, whereas if they are very different, minor diagenesis would be problematic.

Results of the diagenetic evaluations are summarized in Table 2. The Sr/Ca ratio studies and scanning electron microscopy suggest that most samples we studied are completely unrecrystallized. Furthermore, in the case of samples from sites 516 and

593, the strontium isotope ratios of pore waters and coexisting foraminifera are so similar that minor recrystallization would not have affected the foraminiferal composition.

Foraminifera from depths of 110.7 to 206.7 m at site 593 have occasional small euhedral calcite crystals on their surfaces reflecting minor recrystallization. Because these crystals represent a very small fraction of the mass of the tests, and because pore water and foraminiferal strontium isotope ratios are nearly identical, we consider the $^{87}\text{Sr}/^{86}\text{Sr}$ ratios of these samples to be effectively unaltered.

Samples from sites 305 (>60 million years old) and 366 (44 to 60 million years old) are more problematic. Samples from the latter appear well preserved in scanning electron microscopy, but show anomalously low Sr/Ca ratios (Fig. 1). Samples older

than 61 million years in site 305 are cemented on the surface. Their Sr/Ca ratios also appear anomalously low, but for the samples older than 65 million years there are no other Sr/Ca results for comparison. The Delaney curve (26) is complete to 100 million years, but also uses samples from site 305 to define the Cretaceous Sr/Ca record. The $^{87}\text{Sr}/^{86}\text{Sr}$ ratios at both sites 305 and 366 may thus have been changed by recrystallization. Strontium isotope values for these samples therefore are not definitive for use in geochronology, but are probably useful in defining the general shape of the seawater strontium isotope curve. The $^{87}\text{Sr}/^{86}\text{Sr}$ ratios from site 366 are in good agreement with those of well-preserved, age-overlapping samples from site 305, indicating that diagenesis has not greatly changed the original ratios.

Our measured $^{87}\text{Sr}/^{86}\text{Sr}$ ratios are given in

Table 2. Isotopic, chemical and scanning electron microscopy (S) data for all DSDP foraminifera samples.

Core section interval	Age ($\times 10^6$ years)	Depth (m)	Ratio*	$\delta^{87}\text{Sr}\dagger$	Sr/Ca‡ ($\times 10^3$)	S§	Core section interval	Age ($\times 10^6$ years)	Depth (m)	Ratio*	$\delta^{87}\text{Sr}\dagger$	Sr/Ca‡ ($\times 10^3$)	S§
<i>Leg 90, site 593</i>							<i>Leg 68, site 502</i>						
2-6-2-4	0.6	12.6	0.709205 \pm 41	1	1.41	1	1-8-10	0	0.1	0.709204 \pm 32	1	1.29	1
4-CC	1.5	33.9	0.709117 \pm 32	-11	1.39	1	6-3-75-77	1.0	21.9	0.709116 \pm 22	-12	1.27	1
6-CC	2.8	53.1	0.709105 \pm 26	-13	1.40	1	13-1-75-77	2.0	49.6	0.709106 \pm 30	-13	1.30	1
8-CC	3.3	72.3	0.709080 \pm 26	-17	1.34	1	20-1-75-77	3.0	80.4	0.709090 \pm 24	-15	1.12	1
12-CC	3.6	110.7	0.709064 \pm 32	-19	1.36	2	26-3-60-66	4.0	109.6	0.709031 \pm 32	-24	1.18	1
14-CC	3.8	129.9	0.709035 \pm 34	-23	1.36	2	36-1-75-77	5.0	148.9	0.709010 \pm 42	-27	1.15	1
16-CC	4.9	149.1	0.709020 \pm 34	-25	1.32	2	45-1-75-77	6.0	188.5	0.708947 \pm 34	-35	1.12	1
18-CC	6.1	168.3	0.709003 \pm 30	-28	1.28	2	50-1-18-20	7.0	209.8	0.708937 \pm 20	-37	1.30	2
20-CC	7.4	187.5	0.708988 \pm 24	-30	1.30	2							
22-CC	8.6	206.7	0.708974 \pm 30	-32	1.28	2							
24-CC	9.9	225.9	0.708949 \pm 28	-35	1.40	1							
26-CC	11.1	245.1	0.708917 \pm 22	-40	1.30	1	1-1-22-24	21.3	169.3	0.708318 \pm 12	-124	1.28	1
28-CC	12.2	264.3	0.708961 \pm 26	-33	1.38	1	2-1-124-126	22.0	179.9	0.708382 \pm 16	-115	1.32	1
30-5-1-2	12.5	279.9	0.708969 \pm 26	-32	1.39	1	4-1-130-132	23.2	198.9	0.708265 \pm 34	-132	1.30	1
32-CC	13.0	302.7	0.708910 \pm 36	-41	1.41	1	5-1-110-112	23.7	208.2	0.708169 \pm 24	-145	1.34	1
34-5-1-2	13.4	318.3	0.708868 \pm 28	-47	1.41	1	6-2-26-28	24.1	218.4	0.708244 \pm 24	-135	1.21	1
36-CC	13.9	341.1	0.708911 \pm 36	-40	1.36	1	7-3-30-32	24.5	229.4	0.708274 \pm 24	-130	1.34	1
38-CC	14.3	360.3	0.708876 \pm 30	-45	1.39	1	10-1-73-75	25.4	255.3	0.708139 \pm 24	-149	1.30	1
40-CC	14.7	379.5	0.708848 \pm 24	-49	1.26	1	12-1-11-13	26.0	273.7	0.708115 \pm 16	-153	1.27	1
42-3-70-72	15.1	392.8	0.708802 \pm 14	-56	1.35	1	13-3-125-127	26.5	287.4	0.708111 \pm 20	-153	1.30	1
42-CC	16.1	398.7	0.708698 \pm 24	-71	1.35	1	15-3-20-22	27.1	305.8	0.708069 \pm 16	-159	1.40	1
44-1-35-37	17.1	408.7	0.708637 \pm 16	-79	1.28	1	18-1-20-22	28.0	330.8	0.708060 \pm 22	-160	1.36	1
44-CC	18.0	417.9	0.708557 \pm 20	-90	1.35	1	19-2-52-54	28.4	342.1	0.708041 \pm 18	-163	1.36	1
46-1-35-37	19.0	427.9	0.708515 \pm 32	-96	1.37	1	22-1-20-22	29.7	368.8	0.708076 \pm 26	-158	1.40	1
46-CC	19.9	437.1	0.708515 \pm 24	-96	1.35	1	25-2-50-52	31.4	399.1	0.707961 \pm 26	-174	1.39	1
48-CC	21.0	456.3	0.708446 \pm 20	-106	1.36	1	27-3-50-52	32.2	419.2	0.707987 \pm 20	-171	1.41	1
50-CC	23.8	475.5	0.708211 \pm 28	-139	1.39	1	29-3-50-52	33.0	438.6	0.707991 \pm 14	-170	1.41	1
52-2-35-37	26.6	487.0	0.708161 \pm 12	-146	1.32	1	32-3-75-77	34.1	467.4	0.707866 \pm 20	-188	1.36	1
52-4-35-37	27.2	490.0	0.708159 \pm 28	-147	1.35	1	33-4-50-52	34.6	478.1	0.707868 \pm 22	-188	1.37	1
52-CC	28.3	494.7	0.708145 \pm 32	-148	1.39	1	36-3-95-97	35.7	505.6	0.707860 \pm 26	-189	1.30	1
53-3-35-37	29.1	498.1	0.708003 \pm 16	-169	1.35	1	37-3-91-93	36.1	515.0	0.707836 \pm 28	-192	1.34	1
54-1-35-37	30.6	504.7	0.708027 \pm 28	-165	1.35	1	39-3-10-12	36.8	533.2	0.707812 \pm 16	-195	1.32	1
54-2-35-37	30.9	506.2	0.708038 \pm 16	-164	1.39	1	45-1-86-88	39.0	588.0	0.707781 \pm 28	-200	1.30	1
54-CC	32.6	513.9	0.708030 \pm 20	-165	1.41	1	49-2-78-80	40.6	627.4	0.707669 \pm 30	-216	1.26	1
55-2-35-37	33.1	516.8	0.707959 \pm 18	-175	1.41	1	51-2-75-77	41.4	646.4	0.707671 \pm 16	-211	1.28	1
56-2-35-37	34.0	525.4	0.707932 \pm 36	-179	1.43	1	55-1-75-77	43.0	682.9	0.707747 \pm 18	-205	1.28	1
56-5-35-36	35.0	529.9	0.707911 \pm 24	-181	1.39	1	58-1-75-77	44.2	711.4	0.707654 \pm 36	-204	1.16	1
56-CC	35.8	533.1	0.707945 \pm 32	-177	1.40	1	62-2-48-50	45.4	740.1	0.707735 \pm 34	-206	1.13	1
57-6-35-37	37.1	540.1	0.707809 \pm 24	-196	1.36	1	66-1-50-52	46.8	773.6	0.707706 \pm 22	-210	1.12	1
58-2-35-37	38.1	544.6	0.707816 \pm 14	-195	1.41	1	71-1-75-77	48.0	801.9	0.707668 \pm 28	-207	1.10	1
60-2-35-37	39.9	563.8	0.707752 \pm 20	-204	1.45	1	73-2-20-22	48.5	816.3	0.707760 \pm 16	-203	1.16	1
60-CC	40.9	571.5	0.707747 \pm 34	-205	1.45	2	74-2-50-52	49.0	825.6	0.707734 \pm 18	-206	1.18	1

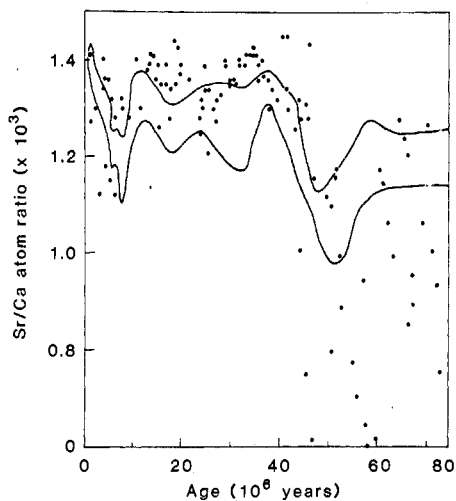


Fig. 1. The Sr/Ca ratios in foraminifera plotted against stratigraphic age. Envelope defines the mean Sr/Ca ratio (80 percent confidence limits) of well-preserved samples as determined by Graham *et al.* (25).

$^{87}\text{Sr}/^{86}\text{Sr}$ of 1×10^{-4} forming a spike-like peak at the Cretaceous/Tertiary boundary.

The data confirm the general shape of the curves defined previously (7, 10, 11), but with important differences. There is a constant offset of about 0.00012 between our curve and that of Burke *et al.* (10), with our strontium isotope ratios being consistently higher. We measured modern seawater and carbonate ratios as 0.709198 ± 0.000020 , which is consistent with strontium isotope ratios measured by other investigators (7, 28), but higher by 0.00013 than those reported by Burke *et al.* The agreement between our curve and those of DePaolo and Ingram (11) and Palmer and Elderfield (7) is excellent with one exception. DePaolo and Ingram reported early Eocene and Paleocene values higher by about 0.00007 than those given here. However, on the basis of a limited number of data points, both curves support the $^{87}\text{Sr}/^{86}\text{Sr}$ increase across the Cretaceous/Tertiary boundary. By contrast, the curve of Burke *et al.* shows considerable scatter in the $^{87}\text{Sr}/^{86}\text{Sr}$ across the boundary.

The evolution of the $^{87}\text{Sr}/^{86}\text{Sr}$ of seawater offers a means to evaluate the global strontium isotope mass balance. Seawater strontium isotope variations with time reflect temporal changes in the mass fluxes of the various sources of strontium to the ocean. Over the long time scale, the $^{87}\text{Sr}/^{86}\text{Sr}$ of seawater and limestones (which derive their strontium from seawater) are fixed simply by the relative fluxes of (continental) crustal strontium and (oceanic) basaltic strontium to the low temperature environment, encompassing seawater and sediments. Since the seawater plus limestone $^{87}\text{Sr}/^{86}\text{Sr}$ is, at

about 0.708, roughly intermediate between that of the continental crust average ($^{87}\text{Sr}/^{86}\text{Sr} = 0.716$) and oceanic basalt ($^{87}\text{Sr}/^{86}\text{Sr} = 0.703$), strontium must be supplied at comparable rates by both mechanisms.

The modern instantaneous strontium isotope balance and its variation through time are more complex, depending on the strontium isotope composition and relative flux from each of the oceanic strontium sources (7, 13, 29). Modeling (7, 29) suggests that in order to explain the major feature of the Cretaceous-Cenozoic isotope record—the long-term increase in the seawater $^{87}\text{Sr}/^{86}\text{Sr}$ ratio—it is necessary to invoke a long-term increase in either the riverine strontium flux or the $^{87}\text{Sr}/^{86}\text{Sr}$ ratio in river strontium going toward the present. Palmer and Elderfield (7) favored the latter possibility; we favor the former (29). Evidence that river fluxes are higher now than during earlier parts of the Cenozoic include the observations that the CaCO_3 compensation depth is at the deepest level for the last 100 million years (30) indicating maximum supply today, the fraction of deep sea floor covered by hiatuses is at a minimum for the present (31), and accumulation rates of various sedimentary components are higher than at any other time during the Cenozoic (31, 32).

One particularly noteworthy feature of the seawater strontium isotope curve is the rapid and monotonic change in the $^{87}\text{Sr}/^{86}\text{Sr}$ between the late Eocene and early Miocene. Our data show that, between 14 and 43 million years ago, the strontium isotope ratio is a single-valued function of time and therefore may be used for correlating and dating marine deposits. The deviation of points from a best-fit straight line drawn through the Oligocene portion of the curve indicates that a sample can be correlated into the strontium isotope stratigraphy with an uncertainty of ± 1 million years. Similar resolution is possible for much of the Miocene. It may also be possible to correlate nearly this well during the Late Cretaceous. On the other hand, strontium isotope variations would not seem useful for late Paleocene-Eocene correlation, or correlation of middle Miocene sediments.

The resolution of strontium isotope stratigraphy is not yet limited by analytical precision. The rate of change of the isotope ratio during the Oligocene, for example, is on the order of 4×10^{-5} per million years; analytical precision is 2×10^{-5} to 3×10^{-5} (2 standard errors) corresponding to an age uncertainty of ± 0.5 to 0.8 million years. The noise in the record probably reflects both minor recrystallization unrecognized by our procedures, and errors in assigned ages due to poor biostratigraphic resolution. We expect the precision of correlation at-

tainable by strontium isotope stratigraphy to improve as better methods are developed for avoiding samples having any diagenetic alteration and as analytical techniques are further improved.

Strontium isotope stratigraphy promises a major contribution in two areas. First, it will generally be the most precise means of correlation during the early Miocene and Oligocene, where the rarity of first appearances and extinctions limit biostratigraphic correlations to a precision of 3 to 4 million years (33-38). Second, it will often be the best correlation tool for largely unfossiliferous marine sediments as well as fossiliferous shallow water deposits that lack age-diag-

Table 3. Isotopic data for pore water samples from DSDP sites 593, 516, and 305.

Core section interval*	Depth (m)	Ratio†
<i>Leg 90, site 593</i>		
Surface seawater		0.709131 \pm 20
1-4	4.8	0.709115 \pm 36
4-3	28.0	0.709063 \pm 22
6-3	47.3	0.709050 \pm 28
8-1	63.5	0.709032 \pm 24
12-3	104.9	0.708967 \pm 18
14-3	124.1	0.708907 \pm 30
16-3	143.3	0.708939 \pm 28
18-3	163.5	0.708952 \pm 22
20-3	181.7	0.708927 \pm 28
22-3	200.9	0.708858 \pm 30
24-3	220.1	0.708883 \pm 32
26-3	239.3	0.708849 \pm 18
28-3	258.5	0.708864 \pm 18
30-3	277.7	0.708806 \pm 20
32-2	296.9	0.708842 \pm 24
34-2	314.6	0.708762 \pm 20
36-2	333.8	0.708745 \pm 18
38-3	354.5	0.708721 \pm 26
40-3	373.7	0.708665 \pm 24
42-3	392.9	0.708629 \pm 14
44-3	412.1	0.708564 \pm 24
46-3	431.3	0.708557 \pm 14
47-3	440.9	0.708532 \pm 14
48-3	450.5	0.708533 \pm 22
50-3	469.7	0.708392 \pm 26
54-2	506.6	0.708345 \pm 14
56-3	527.3	0.708275 \pm 22
58-1	543.5	0.708244 \pm 18
60-3	565.7	0.707945 \pm 18
<i>Leg 72, site 516F</i>		
2-6-140-150	187.6	0.708254 \pm 20
7-2-140-150	229.1	0.708106 \pm 42
13-2-140-150	286.1	0.708091 \pm 28
19-3-140-150	344.6	0.708053 \pm 26
23-3-140-150	401.6	0.707898 \pm 16
30-5-140-150	452.0	0.707866 \pm 34
35-3-140-150	496.6	0.707836 \pm 14
51-1-140-150	648.6	0.707736 \pm 16
<i>Leg 32, site 305</i>		
11-5-144-150	99.0	0.708769 \pm 34
16-5-144-150	146.5	0.708661 \pm 16
21-4-144-150	192.0	0.708684 \pm 22
26-4-144-150	239.0	0.708646 \pm 22

*No intervals were assigned to pore water samples from site 593. †Explanation as in Table 2.

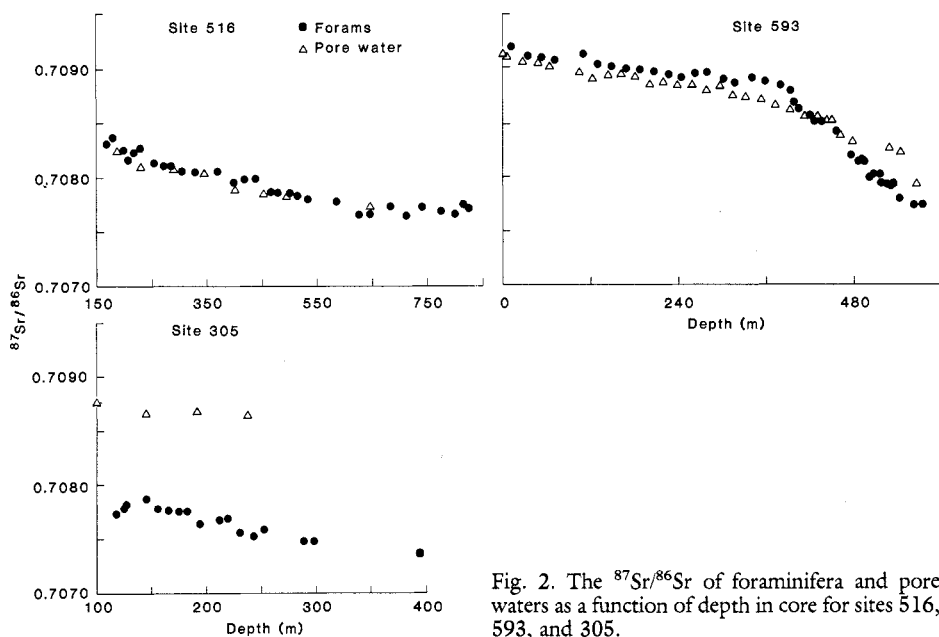


Fig. 2. The $^{87}\text{Sr}/^{86}\text{Sr}$ of foraminifera and pore waters as a function of depth in core for sites 516, 593, and 305.

nostic pelagic microfossils. Strontium isotope stratigraphy provides a new means of high resolution correlation and dating for a wide range of applications. These include correlation of polar and equatorial carbonate sequences, correlation of nearshore and deep-sea carbonate sequences, dating unfossiliferous sediments by the strontium isotope composition of fish debris, and dating authigenic sedimentary phases such as manganese nodules, marine vertebrates, marine phosphorites, and evaporites. We emphasize, however, that no ages should be assigned on the basis of strontium isotope stratigraphy unless the samples have been

thoroughly checked for diagenetic alteration.

Last, we considered whether the measured $^{87}\text{Sr}/^{86}\text{Sr}$ increase of 1×10^{-4} across the Cretaceous/Tertiary (K/T) boundary resulted from the impact of an extraterrestrial object. Iridium anomalies, contemporaneous with mass biological extinctions at the boundary, suggest that the collision of a bolide was responsible for the catastrophic termination of the Mesozoic era (39), although the resulting impact crater has yet to be found (40). A reasonable upper limit on the increase in seawater $^{87}\text{Sr}/^{86}\text{Sr}$ due to a meteorite (chondrite) impact can be calcu-

lated assuming a bolide diameter of 10 km (mass = 10^{18} g) (39), a strontium concentration of 14.5 ppm (41), $^{87}\text{Sr}/^{86}\text{Sr}$ of 0.768 (42), and dissolution of all meteorite strontium in seawater. Under these conditions, the seawater $^{87}\text{Sr}/^{86}\text{Sr}$ rises by only 1×10^{-7} , clearly insufficient to explain the measured spike at the K/T boundary. A bolide diameter of 100 km (1.2×10^{21} g), 10^3 times the mass of the bolide constrained by the iridium anomaly, would be necessary to produce the observed spike.

An alternative scenario is that the considerable energy (about 10^{30} ergs) (43) associated with a large (10 km) bolide impact on the earth would eject 10 to 100 times the bolide mass of rock and water into the stratosphere (43, 44). Ejected particles of 1 μm or less have a sufficiently long residence time in the stratosphere to be globally dispersed (45) before settling back to the earth's surface. The $^{87}\text{Sr}/^{86}\text{Sr}$ of ejecta from an oceanic impact would be low (~ 0.703) reflecting an upper mantle strontium isotope ratio, whereas ejecta derived from a land impact would have a continental crust signature (~ 0.703 to 0.800, depending on the nature and age of the terrain). The increase in the seawater $^{87}\text{Sr}/^{86}\text{Sr}$ ratio of 1×10^{-4} at the K/T boundary raises the question of whether the bolide hit on land, creating a temporary flux of radiogenic strontium from atmospheric dust to the ocean. Mass balance calculations (46) show that 33 to 380 times the bolide mass must be vaporized upon impact and dissolved in the ocean to explain the observed strontium isotope anomaly at the boundary. Varying the strontium concentration and isotopic composition within reasonable limits does not alter this conclusion. O'Keefe and Ahrens (43) suggest that only 0.1 times the bolide mass is ejected in particles of less than 1 μm . Thus we conclude that the current limited estimates of bolide size and vaporization do not favor an impact-derived explanation for the $^{87}\text{Sr}/^{86}\text{Sr}$ increase at the K/T boundary. On the other hand, if the $^{87}\text{Sr}/^{86}\text{Sr}$ increase did result from an impact, the data imply either a larger bolide or higher degree of vaporization than has been suggested.

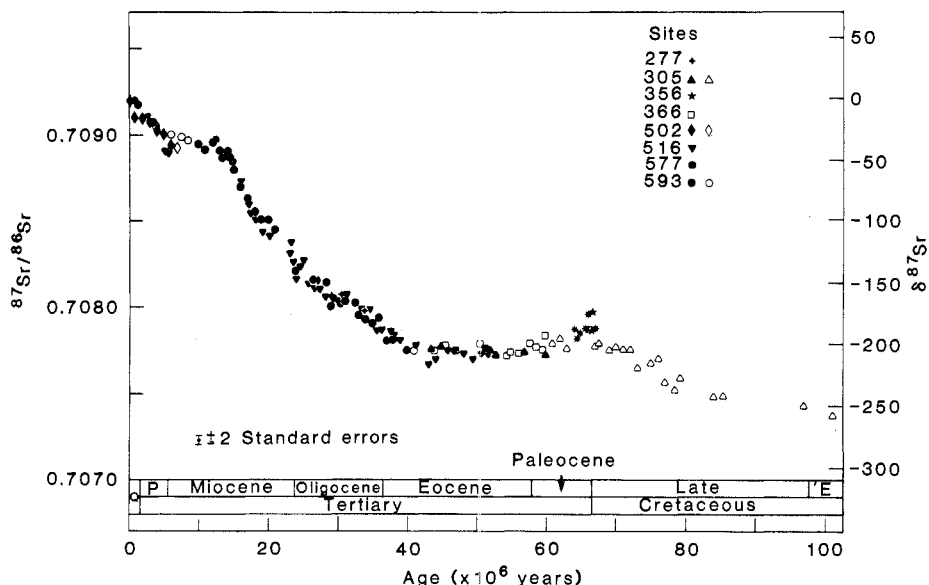


Fig. 3. Measured $^{87}\text{Sr}/^{86}\text{Sr}$ and $\delta^{87}\text{Sr}$ plotted against stratigraphic age (48). Solid symbols represent unrecrystallized samples. Open symbols represent samples with minor recrystallization, cementation, or low Sr/Ca ratios. The $\delta^{87}\text{Sr}$ parameter is defined in the text.

REFERENCES AND NOTES

1. K. K. Turekian, in *Handbook of Geochemistry*, K. H. Wedepohl, Ed. (Springer-Verlag, Heidelberg, 1969), vol. 6, pp. 297-323.
2. W. S. Broecker and T.-H. Peng, *Tracers in the Sea* (Lamont-Doherty Geological Observatory, Palisades, NY, 1982).
3. W. S. Broecker, R. D. Gerard, M. Ewing, B. C. Heezen, in *Oceanography*, M. Sears, Ed. (AAAS Publ. 67, American Association for the Advancement of Science, Washington, DC, 1961), p. 301.
4. E. T. C. Spooner, *Earth Planet. Sci. Lett.* 31, 167 (1976).

5. F. Albarede, A. Michard, J. F. Minster, G. Michard, *ibid.* 55, 229 (1981).
6. J. M. Edmond, K. L. Von Damm, R. E. McDuff, C. I. Measures, *Nature (London)* 297, 187 (1982).
7. M. Palmer and H. Elderfield, *ibid.* 314, 526 (1985).
8. P. A. Baker, J. M. Gieskes, H. Elderfield, *J. Sed. Petrol.* 52, 71 (1982).
9. M. Renard, thesis, University of Paris (1984).
10. W. A. Burke *et al.*, *Geology* 10, 516 (1982).
11. D. J. DePaolo and B. Ingram, *Science* 227, 939 (1985).
12. Z. E. Peterman, C. E. Hedge, H. A. Tourtelot, *Geochim. Cosmochim. Acta* 34, 105 (1970).
13. G. W. Brass, *ibid.* 40, 721 (1976).
14. E. J. Dasch and P. E. Biscaye, *Earth Planet Sci. Lett.* 11, 201 (1971).
15. J. Veizer and W. Compston, *Geochim. Cosmochim. Acta* 38, 1461 (1974).
16. A. Starinsky, M. Bielski, B. Lazar, E. Waksгал, G. Steinitz, *Earth Planet Sci. Lett.* 47, 75 (1980).
17. Sediment samples of approximately 25 cm³ were dried at 50°C, disaggregated in a hot Calgon solution, wet-sieved through a 63-µm screen and dried at 50°C. Whole foraminifera tests (mixed planktonic species; size fraction, 150 µm), were hand-picked. Between 1 and 3 mg of foraminifera were used for isotopic analysis; about 1 mg was dissolved for atomic absorption spectrophotometry. Pore water sample size was 0.5 ml.
18. For isotopic analysis, foraminifera tests were cleaned by repeated sonication in ultrapure water. The cleaned tests were dissolved in 2.5N HCl, and the strontium fraction was separated by cation exchange column. This solution was loaded in a drop of tantalum oxide-phosphoric acid slurry on a single rhenium filament for isotopic analysis. Pore water samples were evaporated to dryness and salts taken up in 2.5N HCl before undergoing the same analytical procedure. Analyses were done at URI on a VG Micromass 30B single collector, double focusing, thermal ionization mass spectrometer. Measured blanks for the procedure are negligible, giving uncertainties less than the in-run errors in Tables 2 and 3 for the 95 percent confidence level. A split of each foraminifera sample was dissolved in dilute HCl and analyzed for strontium and calcium by flameless and flame atomic absorption spectrophotometry, respectively. From these data, Sr/Ca ratios were calculated.
19. W. A. Berggren, D. V. Kent, J. A. Van Couvering, in *Geochronology and the Geological Record*, N. J. Snelling Ed. (Geological Society of London, London, 1985).
20. ———, J. J. Flynn, *ibid.*
21. D. V. Kent and D. J. Spariosu, *Init. Rep. Deep Sea Drill. Proj.* 68, 419 (1982).
22. W. A. Berggren, N. Hamilton, D. A. Johnson, C. Pujol, W. Weiss, P. Cepek, A. M. Gombos, Jr., *ibid.* 72, 939 (1983).
23. H. Elderfield and J. M. Gieskes, *Nature (London)* 300, 493 (1982).
24. H. Elderfield, J. M. Gieskes, P. A. Baker, R. K. Oldfield, C. J. Hawkesworth, R. Miller, *Geochim. Cosmochim. Acta* 46, 2259 (1982).
25. D. W. Graham, M. L. Bender, D. F. Williams, L. D. Keigwin, Jr., *ibid.*, p. 1281.
26. M. L. Delaney, thesis, Massachusetts Institute of Technology (1983).
27. R. B. Lorenz, *Geochim. Cosmochim. Acta* 45, 553 (1982).
28. H. Elderfield and M. J. Greaves, *ibid.* 43, 2201 (1981).
29. J. Hess, M. L. Bender, J.-G. Schilling, *Eos* 61 (No. 46), 1007 (1984); in preparation.
30. T. H. van Andel, G. R. Heath, T. C. Moore, Jr., *Geol. Soc. Am. Mem.* 131, 184 (1975).
31. T. C. Moore, Jr., and G. R. Heath, *Earth Planet. Sci. Lett.* 37, 71 (1977).
32. T. A. Davies, W. W. Hay, J. R. Southam, T. R. Worsley, *Science* 197, 53 (1977); J. R. Southam and W. W. Hay, in *The Sea*, C. Emiliani, Ed. (Wiley, New York, 1981), vol. 7, pp. 1617–1684.
33. R. Cifelli, *Syst. Zool.* 18, 154 (1969).
34. W. A. Berggren, *Micropaleontology* 15, 351 (1969).
35. D. G. Jenkins, in *New Zealand Cenozoic Planktonic Foraminifera*, A. R. Shearer, Ed. (*Paleontological Bulletin* 42, New Zealand Geological Survey, Wellington, 1971).
36. C. H. Ellis, *Init. Rep. Deep Sea Drill. Proj.* 31, 655 (1975).
37. A. R. Edwards and K. Perch-Neilson, *ibid.* 29, 469 (1975).
38. W. H. Blow, *The Cenozoic Globigerinida* (Brill, Leiden, 1979), vol. 3.
39. L. W. Alvarez, W. Alvarez, F. Asaro, H. Michel, *Science* 208, 1095 (1980).
40. R. A. Grieve, *Geol. Soc. Am. Spec. Pap.* 190 (1982), p. 57.
41. K. Gopalan and G. W. Wetherill, in *Handbook in Elemental Abundances in Meteorites*, B. Mason, Ed. (Gordon & Breach, New York, 1971), pp. 297–302.
42. D. A. Papanastassiou, G. J. Wasserburg, D. E. Brownlee, *Earth Planet. Sci. Lett.* 64, 341 (1983).
43. J. D. O'Keefe and T. J. Ahrens, *Geol. Soc. Am. Spec. Pap.* 190 (1982), p. 103.
44. R. M. Schmidt and K. A. Holsapple, *ibid.*, p. 93.
45. O. B. Toon, J. B. Pollack, T. P. Ackerman, R. P. Turco, C. P. McKay, M. S. Liu, *ibid.*, p. 187.
46. Mass balance calculations involved mixing meteoritic and vaporized crustal strontium into the volume of the ocean, and then calculating the change in the seawater ⁸⁷Sr/⁸⁶Sr. End member cases considered were (i) 0.1 times bolide mass of crustal material vaporized (43), and (ii) 10 times bolide mass of crustal material vaporized. We assumed full solubility and dispersal of vaporized meteoritic and crustal strontium in seawater; a bolide size (39) of 10¹⁸ g; strontium in ocean (2), 87 × 10⁻⁶ mol/kg; volume of ocean (2), 1.37 × 10²¹ liters; ⁸⁷Sr/⁸⁶Sr of Late Cretaceous ocean, 0.707865; ⁸⁷Sr/⁸⁶Sr of continental dust, 0.722 (average crust) and 0.800 (upper limit); strontium in upper continental crust (47), 350 µg/g. Resulting model predictions for the increase in seawater ⁸⁷Sr/⁸⁶Sr are (i) average crustal ⁸⁷Sr/⁸⁶Sr, 0.0000003; upper limit ⁸⁷Sr/⁸⁶Sr, 0.0000003; (ii) average crustal ⁸⁷Sr/⁸⁶Sr, 0.0000026; upper limit, 0.000030. The observed change is about 0.0001.
47. S. R. Taylor and S. M. McLennan, *Phil. Trans. R. Soc. London* A301, 381 (1981).
48. ⁸⁷Sr/⁸⁶Sr values plotted for site 516F are 1 to 2 million years too old. Correct ages are given in Table 2.
49. We thank P. Delaney, P. A. Baker, J. P. Kennett, J. Zachos, and the Deep Sea Drilling Project for samples; H. Elderfield and J. Gieskes for encouragement during the early stages of this work; R. Matthews and K. Turekian for discussions on the K/T boundary; R. Kingsley, B. Hannan, M. Cole, G. Waggoner for assistance with mass spectrometry; and R. B. Beach for assistance in the preparation of this manuscript. Supported by NSF grants OCE82-07787 and -8501916.

7 May 1985; accepted 6 January 1986

Evidence for the Involvement of *GM-CSF* and *FMS* in the Deletion (5q) in Myeloid Disorders

MICHELLE M. LE BEAU,* CAROL A. WESTBROOK, MANUEL O. DIAZ, RICHARD A. LARSON, JANET D. ROWLEY, JUDITH C. GASSON, DAVID W. GOLDE, CHARLES J. SHERR

By *in situ* chromosomal hybridization, the *GM-CSF* and *FMS* genes were localized to human chromosome 5 at bands q23 to q31, and at band 5q33, respectively. These genes encode proteins involved in the regulation of hematopoiesis, and are located within a chromosome region frequently deleted in patients with neoplastic myeloid disorders. Both genes were deleted in the 5q- chromosome from bone marrow cells of two patients with refractory anemia and a del(5)(q15q33.3). The *GM-CSF* gene alone was deleted in a third patient with acute nonlymphocytic leukemia (ANLL) who has a smaller deletion, del(5)(q22q33.1). Leukemia cells from a fourth patient who has ANLL and does not have a del(5q), but who has a rearranged chromosome 5 that is missing bands q31.3 to q33.1 [ins(21;5)(q22;q31.3q33.1)] were used to sublocalize these genes; both genes were present on the rearranged chromosome 5. Thus, the deletion of one or both of these genes may be important in the pathogenesis of myelodysplastic syndromes or of ANLL.

COLONY-STIMULATING FACTORS (CSF's) are required for the growth and maturation of myeloid progenitor cells *in vitro* (1, 2). The CSF's are classified according to their cell specificity; hematopoietic progenitor cells respond to CSF's by producing different types of mature blood cells. For example, in the murine system, multi-CSF (IL-3) stimulates the progenitor cells of most of the hematopoietic cell lineages (3), whereas GM-CSF stimulates the proliferation of cells from the granulocyte, granulocyte/macrophage, and macrophage lineages (4). M-CSF (CSF-1) (5) and G-CSF (6) primarily stimulate cells committed to the macrophage and granulocyte lineages, respectively. Human GM-CSF has been purified from medium conditioned by a T-lymphoblast cell line (7), and complementary DNA (cDNA) clones were isolated from an expres-

sion library prepared from messenger RNA (mRNA) (8). The purified recombinant GM-CSF has all of the biological properties attributed to natural GM-CSF (9). More recently, genomic sequences encoding human GM-CSF have been cloned (10). CSF's exert their effects on hematopoietic cells via specific receptors. At present, the cellular receptors specific for CSF's have not been isolated; howev-

M. M. Le Beau, C. A. Westbrook, M. O. Diaz, R. A. Larson, J. D. Rowley, Joint Section of Hematology/Oncology, Department of Medicine, University of Chicago, Chicago, IL 60637.
J. C. Gasson and D. W. Golde, Division of Hematology/Oncology, School of Medicine, University of California, Los Angeles 90024.
C. J. Sherr, Department of Tumor Cell Biology, St. Jude Children's Research Hospital, Memphis, TN 38105.

*To whom correspondence should be addressed at Box 420.